ELSEVIER

www.elsevier.nl/locate/ica

Inorganica Chimica Acta 295 (1999) 214–221

Inorganica Chimica Acta

Synthesis, structures, and linkage isomerism of (allylbenzylmalonate)platinum(II) complexes

Young-A Lee [a,b], Young Keun Chung [b], Youn Soo Sohn [a,*]

[a] *Inorganic Chemistry Laboratory, Korea Institute of Science and Technology, Seoul 130-650, South Korea*
[b] *Department of Chemistry, Seoul National University, Seoul 151-742, South Korea*

Received 18 March 1999; accepted 9 August 1999

Abstract

New platinum(II) complexes $A_2Pt(ABM)$ (A = triethylphosphine (TEP); A_2 = 2,2-dimethyl-1,3-propanediamine (DMPDA), *trans*-(±)-1,2-diaminocyclohexane (DACH); ABM = allylbenzylmalonate) have been synthesized in aqueous solution and characterized by means of X-ray analysis and multinuclear NMR spectroscopy. The crystal structures of *cis*-$(TEP)_2Pt(ABM)$ (monoclinic $P2_1/n$, $a = 12.179(3)$, $b = 16.869(7)$, $c = 12.870(3)$ Å, $\beta = 93.27(2)°$, $V = 2757(1)$ Å^3, $Z = 4$, $R = 0.0390$) and (DACH)-$Pt(ABM)\cdot 2H_2O$ (triclinic $P\bar{1}$, $a = 7.649(3)$, $b = 14.064(2)$, $c = 19.190(8)$ Å, $\alpha = 98.98(2)$, $\beta = 90.05(3)$, $\gamma = 105.73(2)°$, $V = 1961(1)$ Å^3, $Z = 2$, $R = 0.0455$) have been solved. The platinum atom in both complexes adopts a typical square planar arrangement with each coligand in *cis* positions. In the solid state, the ABM ligand exhibits different chelation modes depending on the coligands: (O,O′)-chelation in the phosphine analog and (O,alkene)-chelation in the amine analogs. For the phosphine complex, the (O,O′)-chelation mode of the ABM ligand is impregnable even in solutions at variable temperatures, probably due to the strong π-bonding between the phosphorus and platinum atoms. However, (diamine)platinum(II) complexes have shown interesting linkage isomerism between the (O,O′)- and (O,alkene)-chelation modes in solutions depending on solvent and temperature.

Keywords: X-ray structures; Linkage isomerism; Platinum(II) complexes; Allylbenzylmalonate ligand; NMR spectroscopy

1. Introduction

Among the properties of the metal complexes involving multidentate ligands, linkage isomerism is increasingly important in inorganic chemistry. It is an expanding field that offers a potential for rational control of important biological molecules [1,2], and the results have been extended beyond the initial studies to such diverse areas as quantum mechanical calculations, molecular switches, isomeric catalysts, the design of therapeutic reagents, the imaging agents in the body, and the separation of diastereomers. Although the coordination mode of multidentate ligands may be vaguely predicted via electronic effect, the coordination selectivity is sensitive to various factors such as central metals, coligands, reaction time, temperature, the solvent properties, etc. [1,3–9]. In some cases, the steric factor may play an important role in determining the relative stability of the linkage isomers [10]. According to our previous work, a unique isomerism between the (O,alkene)- and (O,O′)-chelates was observed for allyl- and diallylmalonatoplatinum(II) complexes, which depends on solvent and temperature [11].

In order to expand the coordination chemistry of platinum(II) complexes, another malonate derivative containing one alkene group, allylbenzylmalonate, has been used as a multidentate anionic ligand for the synthesis of new platinum(II) complexes. The ligand may coordinate to the platinum atom via either mode of (O,O′)-, or (O,alkene)-chelation. Phosphine and amine were employed as a coligand in order to examine the coligand effect on the linkage isomerism. Here we report the synthesis and structures of novel platinum(II) complexes $A_2Pt(ABM)$ (A_2 = phosphine or amine, ABM = allylbenzylmalonate) along with their linkage isomerism dependent on coligand, solvent, and temperature.

* Corresponding author. Tel.: +82-2-958 5081; fax: +82-2-958 5089.
E-mail address: yssohn@kistmail.kist.re.kr (Y.S. Sohn)

0020-1693/99/$ - see front matter
PII: S0020-1693(99)00394-1

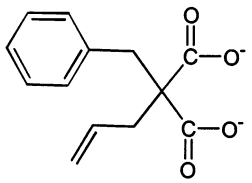

ABM

2. Experimental

2.1. Materials and instrumentation

Potassium tetrachloroplatinate(II) was used as received from Kojima, and triethylphosphine (TEP), 2,2-dimethyl-1,3-propanediamine (DMPDA), and *trans*-(±)-1,2-diaminocyclohexane (DACH) from Aldrich were also used without further purification. Diethyl allylbenzylmalonate (ABM) was prepared by the literature procedure [12] and then hydrolyzed with 1.5 equiv. of $Ba(OH)_2 \cdot 8H_2O$ in 95% methanol to obtain the barium salt. The acid form of ABM was obtained by the standard method [13]. *cis*-Bis(triethylphosphine)-platinum(II) nitrate and *cis*-(diamine)platinum(II) sulfates were also prepared by literature methods [14–16].

Elemental analyses were performed by the Advanced Analysis Center at KIST. The infrared spectra in the 5000–400 cm^{-1} region were measured as KBr pellets on a Perkin–Elmer 16F PC model FT-IR spectrometer. Multinuclear (^1H, ^{13}C, ^{31}P, and ^{195}Pt) NMR spectra were recorded on a Varian Gemini-300 NMR spectrometer operating at 300.00 MHz (^1H), 75.48 MHz (^{13}C), 121.44 MHz (^{31}P) and 64.39 MHz (^{195}Pt) in pulse mode with Fourier transform. Variable temperature ^1H NMR spectra were measured on a Varian Unity Plus 600 MHz NMR spectrometer. The chemical shifts were relative to $SiMe_4$ (^1H and ^{13}C), $(C_6H_5O)_3PO$ (^{31}P), and Na_2PtCl_6 (^{195}Pt) as an internal or external standard for the indicated nuclei.

2.2. Synthesis

2.2.1. *cis*-$(TEP)_2Pt(ABM)$

cis-$(TEP)_2Pt(NO_3)_2$ (2.22 g, 4.0 mmol) dissolved in water (100 ml) was eluted through an anion exchange resin (Amberlite IRA-400 (OH^-)) to obtain a dihydroxy species, *cis*-$(TEP)_2Pt(OH)_2$, and an additional amount of water (400 ml) was passed through the column. To the dihydroxy solution (pH 11.0) was added dropwise an equimolar aqueous solution of H_2ABM (0.94 g, 4.0 mmol) in water (30 ml). The reaction mixture was stirred for 16 h at room temperature (r.t.). The resultant solution was condensed to give a white product in quantitative yield. Recrystallization of the crude product in ethanol–ethyl ether (1:1) afforded colorless crystals suitable for X-ray analysis. Yield 82%. M.p. 136–137°C. *Anal.* Calc. for $C_{25}H_{42}O_4P_2Pt$: C, 45.2; H, 6.38. Found: C, 45.0; H, 6.32%. IR (KBr, cm^{-1}): $\nu(COO)_{asym}$, 1646, 1616; $\nu(COO)_{sym}$, 1360, 1346. ^1H NMR (Me_2SO-d_6, ppm): 1.04 (t, CH_3, 9H, $J = 7.8$ Hz), 1.10 (t, CH_3, 9H, $J = 7.8$ Hz), 1.90 (q, CH_2P, 12H, $J = 7.8$ Hz), 2.49 (d, CH_2, 2H, $J = 6.2$ Hz), 3.42 (s, CH_2, 2H), 4.84 (d, =CH_2, 1H, $J = 17.6$ Hz), 4.91 (d, =CH_2, 1H, $J = 10.2$ Hz), 5.69–5.74 (m, =CH, 1H), 7.11–7.23 (m, C_6H_5, 5H). ^{13}C NMR (Me_2SO-d_6, ppm): 7.6, 13.4, 13.9, 40.0, 42.2, 60.1, 116.5 (C=C), 125.9, 127.5, 129.7, 136.0, 138.3 (C=C), 176.0 (C=O). ^{31}P NMR (Me_2SO-d_6, ppm): 27.7 ($^1J_{Pt-P} = 3536.0$ Hz). ^{195}Pt NMR (Me_2SO-d_6, ppm): −4198.6 ($^1J_{Pt-P} = 7056.5$ Hz).

2.2.2. (DACH)Pt(ABM)

To a solution of $(DACH)PtSO_4 \cdot H_2O$ (0.85 g, 2.0 mmol) in water (50 ml) was added $Ba(ABM) \cdot 2H_2O$ (0.81 g, 2.0 mmol) in water (50 ml), and the resulting mixture was then stirred for 3 h at r.t. After barium sulfate was filtered off, the filtrate was evaporated to dryness. The crude white solid was recrystallized from a mixture of water–acetone (1:1) to obtain colorless crystals suitable for X-ray crystallography (74% yield). M.p. 204°C (dec.). *Anal.* Calc. for $C_{19}H_{26}N_2O_4Pt \cdot H_2O$: C, 40.8; H, 5.04; N, 5.01. Found: C, 40.5; H, 5.00; N, 4.97%. IR (KBr, cm^{-1}): $\nu(COO)_{asym}$, 1664, 1634, 1596, 1564; $\nu(COO)_{sym}$, 1374, 1318, 1290, 1254, 1242. ^1H NMR (D_2O, ppm): 1.10–1.48 (m, 8H), 1.54–1.72 (m, 6H), 1.96–2.04 (m, 2H), 2.07–2.18 (m, 2H), 2.47–2.70 (m, 6H), 2.90 (d, 2H, $J = 13.7$ Hz), 3.25 (d, 2H, $J = 13.4$ Hz), 4.18 (d, 1H, $J = 14.8$ Hz), 4.27 (d, =CH_2, 1H, $J = 14.8$ Hz), 4.74 (d, =CH_2, 1H, $J = 12.4$ Hz), 4.99 (d, =CH_2, 1H, $J = 7.8$ Hz), 5.43–5.67 (q, =CH, 2H), 7.22–7.40 (m, C_6H_5, 10H). ^1H NMR (Me_2SO-d_6, ppm): 0.93–1.09 (m, CH_2 in DACH, 2H), 1.12–1.31 (m, CH_2 in DACH, 2H), 1.39–1.48 (m, CH_2 in DACH, 2H), 1.76–1.89 (m, CH_2 in DACH, 2H), 2.03–2.15 (m, CHN in DACH, 2H), 3.32 (s, CH_2, 2H), 3.66 (dd, CH_2, 2H, $J = 13.3/10.5$ Hz), 4.89 (s, =CH_2, 1H), 4.94 (d, =CH_2, 1H, $J = 4.7$ Hz), 5.13–5.31 (m, NH, 2H), 5.72–5.99 (m, =CH and NH, 3H), 7.04–7.26 (m, C_6H_5, 5H).

2.2.3. (DMPDA)Pt(ABM)

This compound was prepared in 72% yield by the same procedure used for (DACH)Pt(ABM). M.p. 171°C (dec.). *Anal.* Calc. for $C_{18}H_{26}N_2O_4Pt \cdot 2H_2O$: C, 38.2; H, 5.35; N, 4.95. Found: C, 38.2; H, 5.30; N, 4.97%. IR (KBr, cm^{-1}): $\nu(COO)_{asym}$, 1630, 1574; $\nu(COO)_{sym}$, 1284, 1238. ^1H NMR (D_2O, ppm): 0.98 (s, CH_3, 3H), 0.99 (s, CH_3, 3H), 1.71 (dd, CH_2, 1H, $J = 13.2/7.6$ Hz), 2.29 (s, CH_2N, 2H), 2.61–2.78 (m, CH_2 and CH_2N, 3H), 2.93 (d, CH_2, 1H, $J = 13.8$ Hz), 3.28 (d, CH_2, 1H, $J = 13.8$ Hz), 4.25 (d, =CH_2, 1H,

$J = 15.0$ Hz), 4.66 (d, =CH_2, 1H, $J = 7.7$ Hz), 5.51 (q, =CH, 1H), 7.29–7.43 (m, C_6H_5, 5H). ^{1}H NMR (DMF-d_7, ppm): 0.94 (s, CH_3, 6H), 2.34 (s, CH_2N, 4H), 2.63 (d, CH_2, 2H, $J = 6.6$ Hz), 3.67 (s, CH_2, 2H), 4.87–5.00 (m, =CH_2, 2H), 5.37–5.54 (m, NH_2, 4H), 5.86–6.01 (m, =CH, 1H), 7.12–7.33 (m, C_6H_5, 5H). ^{1}H NMR (Me_2SO-d_6, ppm): 0.80 (s, CH_3, 6H), 2.05 (s, CH_2N, 4H), 2.50 (s, CH_2, 2H), 3.63 (s, CH_2, 2H), 4.89 (s, =CH_2, 1H), 4.94 (d, =CH_2, 1H, $J = 7.4$ Hz), 5.21–5.33 (br, s, NH_2, 4H), 5.75–5.89 (m, =CH, 1H), 7.08–7.26 (m, C_6H_5, 5H). ^{1}H NMR (CD_3OD, ppm): (O,O′-isomer); 0.85 (s, CH_3, 3H), 0.87 (s, CH_3, 3H), 3.39 (s, CH_2, 2H), 4.98 (d, =CH_2, 1H, $J = 9.9$ Hz), 5.05 (d, =CH_2, 1H, $J = 17.6$ Hz), 5.71–5.86 (m, =CH, 1H), 7.13–7.39 (m, C_6H_5, 5H), (O,alkene-isomer); 0.94 (s, CH_3, 3H), 0.96 (s, CH_3, 3H), 1.41 (dd, CH_2, 1H, $J = 12.6/7.4$ Hz), 2.58 (dd, CH_2, 1H, $J = 12.7/7.0$ Hz), 3.11 (d, CH_2, 1H, $J = 13.4$ Hz), 3.20 (d, CH_2, 1H, $J = 13.4$ Hz), 4.00 (d, =CH_2, 1H, $J = 14.6$ Hz), 4.43 (d, =CH_2, 1H, $J = 7.7$ Hz), 5.51–5.64 (m, =CH, 1H), 7.13–7.39 (m, C_6H_5, 5H). ^{13}C NMR (D_2O, ppm): 24.0, 26.6, 36.1, 36.2, 44.8, 53.8, 54.2, 68.5, 79.5 (C=C, coordinated to Pt), 98.2 (C=C, coordinated to Pt), 129.6, 129.7, 130.8, 131.1, 133.3, 140.3, 179.1 (C=O, coordinated to Pt), 183.3 (C=O, uncoordinated to Pt). ^{13}C NMR (DMF-d_7, ppm): 23.7, 24.1, 42.0, 44.2, 54.1, 63.3, 115.9 (C=C), 126.4, 128.1, 130.9, 138.3, 140.0 (C=C), 177.5 (C=O). ^{195}Pt NMR (D_2O, ppm): −1162.0. ^{195}Pt NMR (DMF-d_7, ppm): −1944.6. ^{195}Pt NMR (CD_3OD, ppm): −1146.9, −1936.1.

Table 1
Crystallographic data for *cis*-$(TEP)_2$Pt(ABM) and (DACH)-Pt(ABM)·$2H_2O$

	cis-$(TEP)_2$Pt(ABM)	(DACH)Pt(ABM)
Formula	$C_{25}H_{42}O_4P_2Pt$	$C_{38}H_{49}N_4O_8Pt_2 \cdot 2H_2O$
Formula weight	663.62	1116.02
T (°C)	25 (2)	25 (2)
λ (Å)	0.71073	0.71073
Crystal system	monoclinic	triclinic
Space group	$P2_1/n$ (no. 14)	$P\bar{1}$ (no. 2)
a (Å)	12.719(3)	7.649(3)
b (Å)	16.869(7)	14.064(2)
c (Å)	12.870(3)	19.190(8)
α (°)	90.0	98.98(2)
β (°)	93.27(2)	90.05(3)
γ (°)	90.0	105.73(2)
V (Å^3)	2757(2)	1961(1)
Z	4	2
D_{calc} (g cm^{-3})	1.599	1.890
Absorption coefficient (mm^{-1})	5.232	7.189
F(000)	1328	1090
Crystal size (mm)	$0.30 \times 0.35 \times 0.35$	$0.35 \times 0.45 \times 0.30$
θ Range (°)	1.99–24.98	2.15–22.48
Index ranges	$h, k, \pm l$	$h, \pm k, \pm l$
Reflections collected	3824	4520
Independent reflections	3652	4298
Parameters refined	289	477
Goodness-of-fit on F^2	1.092	1.231
Final R indices $[I > 2\sigma(I)]$ [a]	$R_1 = 0.0390$, $wR_2 = 0.0931$	$R_1 = 0.0455$, $wR_2 = 0.1377$

[a] $R_1 = \Sigma||F_o|-|F_c||/\Sigma|F_o|$; $wR_2 = \{\Sigma w(F_o^2 - F_c^2)^2/\Sigma wF_o^4\}1/2$, where $w = 1/\{\sigma^2 F_o^2 + (0.10P)^2 + 0.00P\}$ and $P = \{\max(F_o^2, 0) + 2F_c^2\}/3$.

2.3. X-ray analyses of *cis*-$(TEP)_2$Pt(ABM) and (DACH)Pt(ABM)·$2H_2O$

A single crystal of each compound was wedged in a Lindemann capillary with mother liquor. The X-ray data were collected on an Enraf–Nonius CAD4 automatic diffractometer with graphite-monochromated Mo Kα ($\lambda = 0.71073$ Å) at ambient temperature. Unit cell dimensions were based on 25 well-centered reflections by using a least-squares procedure. During the data collection, three standard reflections monitored every hour did not show any significant intensity variation. The data were corrected for Lorentz and polarization effects. Absorption effects were corrected by the empirical Ψ-scan method. The structures were solved by the Patterson method and were refined by full-matrix least-squares techniques (SHELX-97) [17]. All non-hydrogen atoms were refined anisotropically and hydrogen atoms were added at calculated positions. The largest peak in the final difference synthesis was close to the heavy platinum atom. Crystal parameters and procedural information corresponding to data collection and structure refinement are given in Table 1. See also Section 5.

3. Results

3.1. Synthesis

The reaction of *cis*-bis(triethylphosphine)platinum(II) dihydroxide with allylbenzylmalonic acid in aqueous solution at r.t. smoothly afforded the title complex, *cis*-$(TEP)_2$Pt(ABM), in quantitative yield. The complex is a colorless crystalline solid with a sharp melting point. It is soluble in common organic solvents such as alcohols, chloroform, and dichloromethane, and even slightly soluble in water, but insoluble in ether or hexane. The reaction of (diamine)platinum(II) sulfates with barium salts of the ABM ligand in aqueous solution at r.t. produced the title complexes in high yields (72 ~ 74%) with precipitation of barium sulfate. Recrystallization of the complexes in a solvent pair of water and acetone resulted in colorless crystalline solid products, which decompose in the range of 171 ~ 204°C. The products are moderately soluble in water and in polar organic solvents such as methanol, ethanol, dimethylformamide, Me_2SO, etc., presumably due to the low hydrophilicities of the anionic ligand.

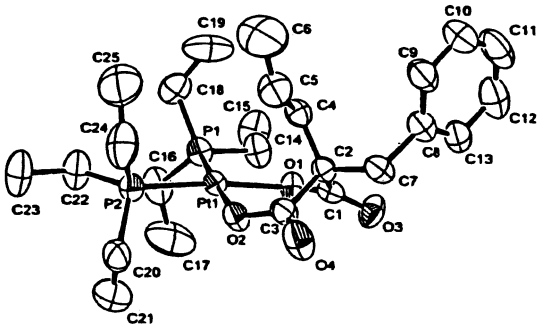

Fig. 1. ORTEP drawing of *cis*-$(TEP)_2Pt(ABM)$ showing the atomic labeling scheme and thermal ellipsoids at the 50% level.

Table 2
Selected bond lengths (Å) and angles (°) for *cis*-$(TEP)_2Pt(ABM)$ and $(DACH)Pt(ABM)\cdot 2H_2O$

cis-$(TEP)_2Pt(ABM)$			
Pt–O(1)	2.059(5)	O(1)–Pt–O(2)	87.2(2)
Pt–O(2)	2.066(5)	O(1)–Pt–P(1)	88.5(2)
Pt–P(1)	2.227(2)	O(2)–Pt–P(2)	84.4(2)
Pt–P(2)	2.234(2)	P(1)–Pt–P(2)	99.87(8)
O(1)–C(1)	1.290(9)	O(4)–C(3)–O(2)	121.5(7)
O(2)–C(3)	1.292(9)	C(1)–C(2)–C(3)	103.8(6)
O(3)–C(1)	1.203(9)	C(8)–C(7)–C(2)	118.8(6)
O(4)–C(3)	1.217(9)	O(3)–C(1)–C(2)	120.4(7)
C(4)–C(5)	1.44(1)	C(6)–C(5)–C(4)	126(1)
C(5)–C(6)	1.33(2)		
$(DACH)Pt(ABM)\cdot 2H_2O$			
Pt(1)–O(1)	1.979(9)	O(1)–Pt(1)–C(8)	90.0(5)
Pt(1)–N(1)	2.02(1)	O(1)–Pt(1)–C(7)	93.0(5)
Pt(1)–N(2)	2.09(1)	O(1)–Pt(1)–N(1)	171.8(3)
Pt(1)–C(8)	2.16(1)	N(1)–Pt(1)–N(2)	84.2(4)
Pt(1)–C(7)	2.17(1)	C(8)–Pt(1)–C(7)	36.1(5)
O(1)–C(11)	1.31(3)	O(1)–C(11)–O(2)	121(1)
O(2)–C(11)	1.21(2)	O(3)–C(12)–O(4)	124(1)
O(3)–C(12)	1.22(2)	C(7)–C(8)–C(9)	124(1)
O(4)–C(12)	1.26(2)		
C(7)–C(8)	1.34(2)		

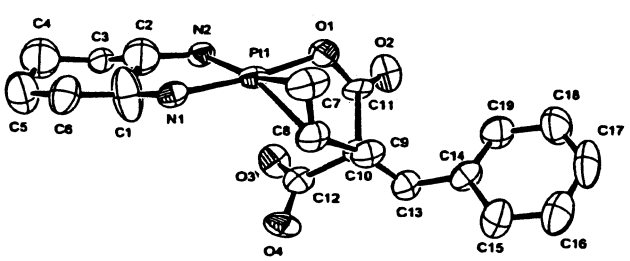

Fig. 2. ORTEP drawing of $(DACH)Pt(ABM)\cdot 2H_2O$ showing the atomic labeling scheme and thermal ellipsoids at the 50% level.

They are stable in aqueous and organic solutions at least for a few weeks at r.t.

3.2. Solid state structures

The X-ray crystal structure of *cis*-$(TEP)_2Pt(ABM)$ is depicted in Fig. 1, and relevant bond distances and angles are listed in Table 2. As expected, the local geometry around the platinum(II) atom approximates to a typical square plane with two phosphorus atoms in *cis* positions. The anionic ABM ligand chelated the platinum atom through two carboxylate groups, resulting in (O,O′)-chelation. The bond lengths of C(1)–O(1) (1.290(9) Å) and C(3)–O(2) (1.292(9) Å) are longer than those of C(1)–O(3) (1.203(9) Å) and C(3)–O(4) (1.217(9) Å), being consistent with typical monodentate carboxylates in other platinum(II) complexes. The C(5)–C(6) distance of the alkene group (1.33(2) Å) is close to that of the normal double bond (1.33 Å) [18]. The bond lengths of Pt–P (2.227(2), 2.234(2) Å) are similar to those of Pt–P bonds in other phosphine–platinum(II) complexes [16]. The angle of P(1)–Pt–P(2) (99.87(8)°) is splayed out due to the steric crowding of triethyl groups on the phosphorus atom. Thus the bulkiness of the phosphine ligand is partially responsible for the distortion of the square planar geometry around the platinum atom.

For $(DACH)Pt(ABM)\cdot 2H_2O$, there are two independent molecules in an asymmetric region of a triclinic unit cell and the structures of the two molecules are within error of being identical. One of the molecules and its labeling scheme are depicted in Fig. 2, and the selected bond distances and angles are listed in Table 2. The local geometry around the platinum(II) atom also approximates to a square plane. However, an interesting feature is the bonding mode of the anionic ABM ligand which chelated the platinum atom through one of the two carboxylate groups (Pt(1)–O(1), 1.979(9) Å) and the alkene group (Pt(1)–C(7), 2.17(1); Pt(1)–C(8), 2.16(1) Å), resulting in (O,alkene)-chelation. Thus another carboxylate group is uncoordinated in contrast to the (O,O′)-chelation mode of *cis*-$(TEP)_2Pt(ABM)$. For the coordinated carboxylate group, the bond length of C(11)–O(1) (1.31(2) Å) is longer than that of C(11)–O(2) (1.21(2) Å). The corresponding bond lengths of the dangling carboxylate group are 1.22(2) (C(12)–O(3)) and 1.26(2) Å (C(12)–O(4)), which indicate the relatively delocalized charge distribution. The C(7)–C(8) bond length of the alkene group (1.34(2) Å) is similar to that of the normal double bond (1.33 Å). The alkene group is positioned perpendicularly to the platinum plane and the C(7)–Pt–C(8) angle of 36.1(5)° is smaller than the values of 40 to 43° observed in other known alkene–platinum(II) complexes [19,20]. Intermolecular hydrogen bonds exist between the carboxylate group and the amine NH (O···N′ distances, 2.79–2.86 Å). These intermolecular hydrogen bonds may give rise to additional stability for the (O,alkene)-chelate in the solid state.

The chelation mode of the anionic ligand in the solid state can also be clearly discerned by the stretching frequencies of the carboxylate groups in the IR spectra [21]. For *cis*-$(TEP)_2Pt(ABM)$, two asymmetric carboxy-

late stretching frequencies at 1646 and 1616 cm^{-1} and two corresponding symmetric stretching frequencies at 1360 and 1346 cm^{-1} indicate that the two carboxylate groups are not equivalent, but the large separation ($\Delta\nu > 270$ cm^{-1}) between the asymmetric and symmetric stretching bands implies that both carboxylates of the ABM ligand are coordinated in a monodentate fashion to the platinum atom, which is in accord with the aforementioned X-ray data. For (DMPDA)-Pt(ABM), two asymmetric carboxylate bands were also observed at 1630 and 1574 cm^{-1}, but the band at 1630 cm^{-1} corresponds to the carboxylate group coordinated to the platinum atom, while the band at 1574 cm^{-1} is due to the uncoordinated carboxylate, which lies in the same region as its free ligand (1568 cm^{-1}). Thus, the IR spectra for (DMPDA)Pt(ABM) disclose coexistence of a coordinated and a dangled carboxylate group, i.e. (O,alkene)-chelation. The spectral similarity of the carboxylate bands of (DACH)Pt(ABM) to that of (DMPDA)Pt(ABM) suggests that the bonding mode of the anionic ligand is not dependent on these kinds of amine coligands.

3.3. Solvent effect

The ^{31}P NMR spectrum of *cis*-$(TEP)_2Pt(ABM)$ in Me_2SO solution exhibits a single signal flanked by ^{195}Pt satellites ($^1J_{Pt-P} = 3536.0$ Hz) at 27.7 ppm, and the ^{195}Pt NMR spectrum shows only a triplet at -4198.6 ppm ($^1J_{Pt-P} = 7056.5$ Hz), which reflects the presence of one platinum species in the solution. Furthermore, these chemical shifts are similar to those of *cis*-$(PMe_3)_2Pt(oxalate)$ (^{31}P NMR (D_2O) $\delta = -26.7$; ^{195}Pt NMR (D_2O) $\delta = -4334$), which were already elucidated as *cis*-(P,P)Pt(O,O) [22]. The ^1H NMR spectra disclose that the allybenzylmalonate group is coordinated to the platinum(II) atom in (O,O′)-chelation mode in various polar solvents such as CD_3OD, Me_2SO, DMF, and D_2O. Thus, for the present phosphine complex, only the (O,O′)-chelate was obtained in the solid state and the (O,O′)-bonding mode of the allybenzylmalonate ligand is retained without dissociation or isomerization in these solutions.

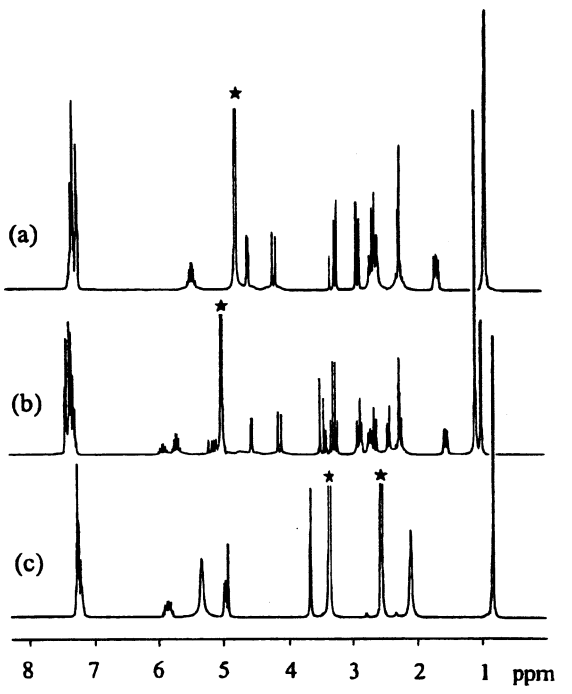

Fig. 3. ^1H NMR spectra of (DMPDA)Pt(ABM) in D_2O (a), CD_3OD (b), and Me_2SO-d_6 (c). The star-marked peaks are due to solvent molecules.

However, for the (diamine)Pt(ABM) complexes, multinuclear (^1H, ^{13}C, and ^{195}Pt) NMR studies have shown that the chelation mode of the anionic ABM ligand is prominently solvent-dependent, in contrast to the above phosphine analog. In D_2O solution, the ^{13}C NMR spectrum of (DMPDA)Pt(ABM) exhibits two resonances at 183.3 and 179.1 ppm, corresponding to a free carboxylate and a coordinated carboxylate, respectively. The alkene resonances at 98.2 and 79.5 ppm are significantly shifted upfield compared to those of the potassium salt of ABM (139.3 and 117.8 ppm). Such results clearly indicate that the (O,alkene)-chelation mode of the ABM ligand is retained in aqueous solution. In DMF solution, however, the ^{13}C NMR spectrum of (DMPDA)Pt(ABM) shows a quite different resonance pattern. The ^{13}C chemical shift of the carboxylate groups shows a single resonance at 176.1 ppm, and the alkene resonances (140.0 and 115.9 ppm) of the ABM ligand are similar to those of its potassium salt. Thus, for (DMPDA)Pt(ABM), the ABM ligand chelates the platinum atom through two carboxylate groups in DMF solution, in contrast to its (O,alkene)-mode in the solid state and in aqueous solution. The ^1H NMR spectra of (DMPDA)Pt(ABM) in different solvents at r.t. are presented in Fig. 3. The $=CH_2$ protons of ABM in D_2O (Fig. 3(a)) show two doublets at 4.66 ($^3J_{trans} = 7.7$ Hz) and 4.25 ($^3J_{cis} = 15.0$ Hz) ppm that shift to higher field compared to those of a free alkene group. The methylene proton resonances of the ABM and DMPDA ligands are complicated due to the unsymmetrical ligation of the ABM ligand, i.e. (O,alkene)-chelation. However, its ^1H NMR spectrum (Fig. 3(c)) in Me_2SO-d_6 is prominently different from that in D_2O. The $=CH_2$ protons of ABM in D_2O (Fig. 3(a)) show a doublet at 4.94 ppm and a singlet at 4.89 ppm, disclosing that the alkene group of the ABM ligand is not coordinated in Me_2SO. The complex has the same bonding mode in DMF as that in Me_2SO. The chemical shifts and the resonance pattern of the complex in CD_3OD (Fig. 3(b)) indicate an equilibrium between the two chelation modes at r.t. For (DACH)Pt(ABM), similar spectral patterns were observed in each solution.

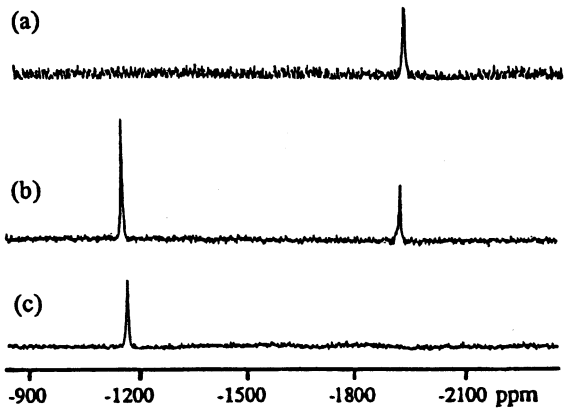

Fig. 4. ^{195}Pt NMR spectra of (DMPDA)Pt(ABM) in DMF-d_7 (a), CD_3OD (b), and D_2O (c).

The ^{195}Pt NMR spectra demonstrate more clearly the structural variation dependent on the solvent. The ^{195}Pt NMR spectra of (DMPDA)Pt(ABM) were measured in various solvents and shown in Fig. 4. The spectrum in DMF solution (Fig. 4(a)) exhibits only one ^{195}Pt resonance, reflecting the presence of one platinum species in the solution. Furthermore, the chemical shift at -1945 ppm in DMF-d_7 lies in a similar region to that of (DMPDA)Pt(DAM) (-1932 ppm), which were already elucidated as (N,N′-DMPDA)Pt(O,O′-DAM) [11]. However, the ^{195}Pt NMR spectrum in CD_3OD (Fig. 4(b)) shows two resonances at -1936 and -1147 ppm with the ratio of approximately 1:2 at r.t., supporting that the two isomers coexist in methanol solution. The signal at -1936 ppm corresponds to the (O,O′)-chelate while the chemical shift at -1147 ppm is assignable to the (O,alkene)-chelate. The ^{195}Pt NMR spectrum in D_2O (Fig. 4(c)) shows a single resonance at -1162 ppm, indicating the presence of only one (O,alkene)-isomer. Thus, for the present platinum complexes, variation of medium significantly affects the coordination mode of the anionic ligand.

3.4. Temperature effect

The proton spectrum of (DMPDA)Pt(ABM) in CD_3OD exhibits a marked temperature dependence in the range of 188–328 K (Fig. 5). The spectrum of (DMPDA)Pt(ABM) in CD_3OD at r.t. (at 298 K) shows two sets of resonance signals, indicating coexistence of the two linkage isomers, (O,O′)- and (O,alkene)-chelates, in the ratio of approximately 1:2. When the solution was cooled down to 188 K, the ratio of two linkage isomers did not change, and only some peaks were broadened. However, warming up the solution resulted in gradual increasing of the (O,alkene)-chelate (indicated as ↓ in Fig. 5), and at 328 K (the limit temperature of CH_3OH), the ratio of the (O,O′)- and (O,alkene)-chelates became approximately 2:1. An

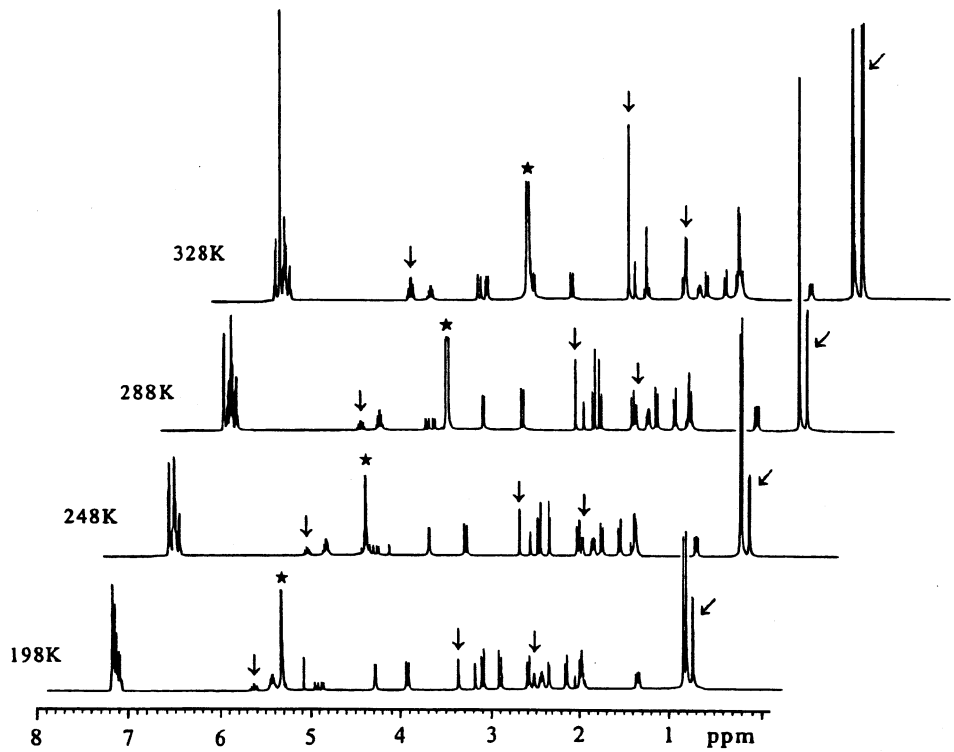

Fig. 5. Variable-temperature ^{1}H NMR spectra of (DMPDA)Pt(ABM) in CD_3OD (500 MHz). The star-marked peak is due to water molecule.

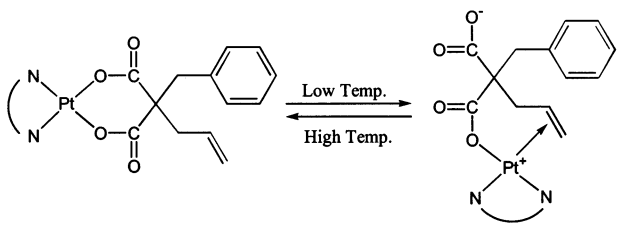

interesting feature is that such a switching is essentially reversible on temperature: at low temperature the ABM ligand has a chelation mode of (O,alkene) whereas at elevated temperature the equilibrium shifts to the (O,O′)-chelate. For the phosphine analog such a linkage isomerism was not observed and only the (O,O′)-chelation mode was locked in the temperature range of 188 to 340 K.

4. Discussion

Structural characterization of the platinum(II) complexes containing the ABM ligand has shown that different linkage isomers were observed that depended on the subtle change of various factors. Different bonding fashions of the anionic ABM ligand were clearly observed depending on different coligands: the ABM complexes have shown (O,O′)- and (O,alkene)-chelation modes in the solid state with phosphine and amine coligands, respectively. Such a difference between the chelation modes seems to be due to the stabilization induced by the electronic effect of the coligands. The phosphine ligand is known to form a strong π bond with transition metals by back-donation (dπ–dπ) [23]. Therefore, it is presumed that the back-donation from the two phosphorus atoms ($3d_{xz}$, $3d_{yz}$) to the platinum atom ($5d_{xz}$, $5d_{yz}$) excludes π-bonding by the alkene group. Such a strong electronic effect seems to be superior to the solvent and temperature effects, and consequently, only (O,O′)-chelation mode is locked for the (diphosphine)platinum(II) complex.

However, for the amine analogs without competition for π-bonding (amine can not form a π bond), the ethylene group is preferentially bonded. Moreover, the intermolecular hydrogen bonds between the carboxylate and amine NH groups may give rise to additional stability for (O,alkene)-chelation in the solid state. In solutions, the present ABM complexes exhibit linkage isomerism between the (O,O′)- and (O,alkene)-chelates similarly to the allyl- and diallylmalonate complexes previously reported [11], and the hydrogen bonding ability of solvent with the platinum complex molecules seems to play an important role in controlling the coordination mode of the ABM ligand. The (O,alkene)-chelated species has a zwitterionic form, which interacts with the solvent molecules through hydrogen bonding. Therefore, it appears that the (O,alkene)-mode is more stable in the protic solvent, whereas the (O,O′)-mode is relatively more stable in aprotic solvents such as Me_2SO and dimethylformamide. Such a result proves that solvent molecules play an important role in the determination of the coordination mode. In polarity, dielectric constant, and hydrogen bonding ability, MeOH is a medium between the two extremes, H_2O and Me_2SO, and as such the two chelation modes coexist in MeOH solution, its equilibrium being dependent on temperature. Temperature-dependent NMR spectra have been used to determine the transition temperature and reversibility. For instance, (DMPDA)Pt(ABM) in CD_3OD exhibited an equilibrium between the two species at r.t., but warming up the sample, the (O,O′)-mode is favored because the hydrogen bonding is weakened at high temperature. This result is an evidence for the stabilization by hydrogen bonding. For the (diamine)-platinum complexes, the two chelation modes seem to be energetically close to each other.

In conclusion, it has been shown in this study that the electronic effect of the coligand on the linkage isomerism was dominant compared with the solvent and temperature effects. However, solvent and temperature are also important in controlling the linkage isomerism that may be useful in molecular control. In particular, the interconversion properties between the (O,O′)- and (O,alkene)-modes appear to be associated with proximity in energy between the two chelation modes of the allylbenzylmalonate ligand. Various factors should be understood prior to molecular design of new platinum compounds that exhibit desirable molecular properties.

5. Supplementary material

Details of atomic coordinates, anisotropic thermal parameters, lists of bond lengths and angles, and ^{13}C NMR spectra of (DMPDA)Pt(ABM) are supplied. Additional information, such as final atomic coordinates and isotropic thermal parameters of *cis*-$(TEP)_2$-Pt(ABM) and (DACH)Pt(ABM)·$2H_2O$, is available from the author on request.

Acknowledgements

This research was financially supported by the Ministry of Science and Technology in Korea.

References

[1] (a) T.G. Appleton, F.J. Pesch, M. Wienken, S. Menzer, B. Lippert, Inorg. Chem. 31 (1992) 4410. (b) N. Farrell, Transition

Metal Complexes as Drugs and Chemotherapeutic Agents, Kluwer, Dordrecht, 1989. (c) W.J.F. Van der Vijgh, Clin. Pharmacokinet. 21 (1991) 242.
[2] H.A. Ankersmit, P.T. Witte, H. Kooijman, M.T. Lakin, A.L. Spek, K. Goubitz, K. Vrieze, G. van Koten, Inorg. Chem. 35 (1996) 6053.
[3] A.M.M. Lanfredi, F. Ugozzoli, A. Camus, N. Marsich, R. Capelletti, Inorg. Chim. Acta 206 (1993) 173.
[4] D.A. Buckingham, Coord. Chem. Rev. 135/136 (1994) 587.
[5] C.A. Bignozzi, C. Chiorboli, M.T. Indelli, F. Scandola, V. Bertolasi, G. Gilli, J. Chem. Soc., Dalton Trans. (1994) 2391.
[6] D. Das, N.R. Chaudhuri, A. Ghosh, Polyhedron 15 (1996) 3919.
[7] T. Parac, N.M. Kostic, J. Am. Chem. Soc. 118 (1996) 5946.
[8] L. Piao, F. Kai, M. Nirohata, Y. Matsuoka, H. Huang, Polyhedron 15 (1996) 3107.
[9] (a) G.R. Clark, G.J. Palenik, Inorg. Chem. 9 (1970) 2754. (b) J.L. Burmeister, N.J. DeStefano, J. Chem. Soc., Chem. Commun. (1970) 1968.
[10] (a) J.L. Burmeister, N.J. DeStefano, Inorg. Chem. 8 (1969) 1546. (b) J.L. Burmeister, J.C. Lim, J. Chem. Soc., Chem. Commun. (1969) 1154.
[11] (a) Y.-A Lee, Y.K. Chung, K.M. Kim, Y.S. Sohn, Inorg. Chim. Acta 279 (1998) 116. (b) Y.-A. Lee, Y.K. Chung, Y.S. Sohn, Inorg. Chem. 38 (1999) 531.
[12] C.S. Marvel, Org. Synth., Coll. III (1955) 705.
[13] B.S. Furniss, A.J. Hannaford, P.W.G. Smith, A.R. Tatchell, Vogel's Textbook of Practical Organic Chemistry, Longman Scientific and Technical, London, 1989, p. 680.
[14] G.L. Johnson, Inorg. Synth. 8 (1966) 242.
[15] O. Gandolfi, H.C. Apfelbaum, J. Blum, Inorg. Chim. Acta 135 (1987) 27.
[16] (a) H. Yuge, T.K. Miyamoto, Chem. Lett. (1996) 375. (b) H. Kawai, Y. Kitano, M. Mutoh, G. Hata, Chem. Pharm. Bull. 41 (1993) 357.
[17] G.M. Sheldrick, SHELX-97, A Program for Structure Determination and Refinement, University of Göttingen, Germany, 1997.
[18] R.T. Morrison, R.N. Boyd, Organic Chemistry, third ed., Allyn and Bacon, Boston, MA, 1973, p. 145.
[19] M.A. Bennett, J.C. Jeffery, G.B. Robertson, Inorg. Chem. 18 (1979) 1071.
[20] L.E. Erickson, G.S. Jones, J.L. Blanchard, K.J. Ahmed, Inorg. Chem. 30 (1991) 3147.
[21] J.D. Hoeschele, N. Farrel, W.R. Turner, C.D. Rithner, Inorg. Chem. 27 (1988) 4106.
[22] T.K. Miyamoto, Y. Suzuki, Bull. Chem. Soc. Jpn. 65 (1992) 3386.
[23] F.A. Cotton, G. Wilkinson, Advanced Inorganic Chemistry, fourth ed., Wiley, New York, 1980, p. 88.